The Journal of Chemical Physics

Three-step colloidal gelation revealed by time-resolved x-ray photon correlation spectroscopy

Cite as: J. Chem. Phys. **157**, 184901 (2022); https://doi.org/10.1063/5.0123118
Submitted: 28 August 2022 • Accepted: 18 October 2022 • Accepted Manuscript Online: 18 October 2022 • Published Online: 08 November 2022

Published open access through an agreement with DESY

Avni Jain, Florian Schulz, Francesco Dallari, et al.

AIP Publishing

The Journal of Chemical Physics ARTICLE scitation.org/journal/jcp

Three-step colloidal gelation revealed by time-resolved x-ray photon correlation spectroscopy

Cite as: J. Chem. Phys. 157, 184901 (2022); doi: 10.1063/5.0123118
Submitted: 28 August 2022 • Accepted: 18 October 2022 •
Published Online: 8 November 2022

Avni Jain,[1,a] Florian Schulz,[2,3] Francesco Dallari,[1,b] Verena Markmann,[1,c] Fabian Westermeier,[1] Yugang Zhang,[4] Gerhard Grübel,[1,3,d] and Felix Lehmkühler[1,3,e]

AFFILIATIONS

[1] Deutsches Elektronen-Synchrotron DESY, Notkestr. 85, 22607 Hamburg, Germany
[2] Institute of Nanostructure and Solid State Physics, University of Hamburg, Luruper Chaussee 149, 22761 Hamburg, Germany
[3] The Hamburg Centre for Ultrafast Imaging, Luruper Chaussee 149, 22761 Hamburg, Germany
[4] Center for Functional Nanomaterials, Brookhaven National Laboratories, Upton, New York 11973, USA

Note: This paper is part of the JCP Special Topic on Colloidal Gels.
[a] **Current address:** Blue Yonder GmbH, Oberbaumbrücke 1, 20457 Hamburg, Germany.
[b] **Current address:** Dipartimento di Fisica e Astronomia, "Galileo Galilei," Università degli Studi di Padova, Via F. Marzolo 8, 35131 Padova, Italy.
[c] **Current address:** Technical University of Denmark, Fysikvej 307, 2800 Lyngby, Denmark.
[d] **Current address:** European X-ray Free-Electron Laser, Holzkoppel 4, 22869 Schenefeld, Germany.
[e] **Author to whom correspondence should be addressed:** felix.lehmkuehler@desy.de

ABSTRACT

The gelation of PEGylated gold nanoparticles dispersed in a glycerol–water mixture is probed *in situ* by x-ray photon correlation spectroscopy. Following the evolution of structure and dynamics over 10^4 s, a three-step gelation process is found. First, a simultaneous increase of the Ornstein–Zernike length ξ and slowdown of dynamics is characterized by an anomalous q-dependence of the relaxation times of $\tau \propto q^{-6}$ and strongly stretched intermediate scattering functions. After the structure of the gel network has been established, evidenced by a constant ξ, the dynamics show aging during the second gelation step accompanied by a change toward ballistic dynamics with $\tau \propto q^{-1}$ and compressed correlation functions. In the third step, aging continues after the arrest of particle motion. Our observations further suggest that gelation is characterized by stress release as evidenced by anisotropic dynamics once gelation sets in.

I. INTRODUCTION

Soft matter systems, such as colloidal particles dispersed in a liquid, are known to show a rich phase behavior, covering multiple crystalline, glass, and gel states.[1–4] Following their structure and dynamics *in situ* during phase transitions and state changes represents a main subject of soft matter physics. Although often referred to as model systems, colloidal dispersions may show very complex dynamics, such as dynamical heterogeneities due to particle caging, localization as well as cooperative particle movements.[5–7] In particular, this applies to the formation process of colloidal gels.[8–10] This gelation process is driven by spinodal decomposition forming two phases of different viscosity,[2,9,11–15] typically resulting in heterogeneous dynamics. Afterward, the high-viscosity phase percolates.[16–19] The gelation continues over longer times undergoing aging.[20–22]

Due to their sensitivity to slight changes of experimental parameters, studies on the structure, dynamics, and properties of colloidal gels during formation and aging are challenging. In particular, experimental techniques are needed that provide the necessary time (μs to h) and spatial (few to 100 s of nm) resolution to track gelation, covering all characteristic time scales from diffusion to arrested particles on the relevant interparticle length scales. In recent years, x-ray photon correlation spectroscopy (XPCS) has been developed to meet these criteria,[23–30] offering real-time probes of kinetics and dynamics down to sub-nm length scales. In particular, XPCS enables studying dynamic heterogeneities at relevant length scales, including

interparticle distances as well as clusters formed by many particles. Recently, XPCS was used to measure the kinetics of liquid–liquid phase separations[31] and network formation in proteins.[32] While both processes cover aspects of gelation, our understanding of the structure and dynamics of this process is largely incomplete.

Here, we report on the structure and dynamics of colloidal suspension of PEGylated gold nanoparticles dispersed in a glycerol–water mixture while undergoing gelation. Tracking the structure and dynamics by small-angle x-ray scattering (SAXS) and XPCS during cooling below the gelation temperature, we find a three-step gelation process. This is first characterized by a simultaneous increase in the characteristic length scale and slowdown of dynamics by more than four orders of magnitude. Increasingly anisotropic and anomalous dynamics are found. After the structural change has finished, the dynamics show aging, where the relaxation time slows down continuously, accompanied by a change toward ballistic dynamics with $\tau \propto q^{-1}$ and compressed correlation functions. Finally, aging continues over the whole experimental time window.

II. EXPERIMENTAL

A. Sample details

The gelation process was studied for gold nanoparticles (AuNP) coated with α-methoxypoly(ethylene glycol)-ω-(11-mercaptoundecanoate) (PEGMUA, 5 kDa) dispersed in a mixed solvent of glycerol and water (70:30 v/v). The synthesis of such PEGylated particles has been reported elsewhere.[33,34] The radius of the gold nanoparticles was about 6.1 nm with a size dispersity of less than 10% as confirmed by transmission electron microscopy (TEM) and dynamic light scattering (DLS), the ligand length is about 10–14 nm in pure water.[35] More details on sample characterization are shown in the supplementary material. The volume fraction of the particles was ~5 vol. %. Such dispersions have been reported previously to form colloidal gels below a weakly concentration-dependent temperature around $T_{gel} \sim 280$ K.[22] For $T < T_{gel}$, the particle interactions become attractive, promoting network formation and thus gelation.

B. Coherent x-ray scattering experiments

The XPCS experiments have been performed at beamlines CHX (11-ID) of NSLS-II at Brookhaven National Laboratory (Upton, NY, USA) and P10 of PETRA III at DESY (Hamburg, Germany). At CHX, we used a small-angle x-ray scattering setup with a sample–detector distance of 16 m. The x-ray energy was 9.6 keV, the beam was focused to about 10×10 μm^2. At P10, the ultrasmall-angle x-ray scattering (USAXS) geometry was used, where the detector was placed 21.2 m downstream from the sample position. The beam energy was 8.1 keV and its size was set to 100×100 μm^2 using slits. This USAXS geometry allows partial overlapping of the accessible q-range with light scattering studies[10,20,36] without the experimental limitations of visible light, e.g., multiple scattering. At both beamlines, capillaries filled with the samples were placed into a temperature-controllable sample holder that was evacuated afterward. Series of typically 1000–5000 speckle patterns were measured with exposure times per pattern down to 1.4 ms, which corresponds to the maximum achievable frame rate of 750 Hz of the Eiger X4M detector used at both beamlines. The gelation temperature was obtained by performing stepwise cooling and measurement between room temperature and 270 K and found to be around 276 K. Afterward, a fresh sample from the same batch was cooled down to 272 K, i.e., below the gelation temperature, at a cooling rate of 1 K/min. During cooling, XPCS runs were continuously performed cycling over 10 different spots on the sample to reduce the dose per sample spot. The first measurement started at $t_w = 0$ s and the last one concluded after about $t_w = 10^4$ s. The data were tracked in real time to adapt the exposure times and length of the series to cover the dynamics in all sample states. To keep the x-ray dose constant, the x rays were attenuated for longer exposure times. Here, we discuss the results for a sample at a volume fraction of 5 vol. %, similar results have been obtained for 7 vol. % and 10 vol. %.

In XPCS experiments, sample dynamics are obtained by autocorrelations of the speckle patterns, i.e., diffraction patterns in a coherent x-ray scattering experiment, given by[37–40]

$$g_2(q,t) = \frac{\langle I(q,t')I(q,t'+t)\rangle_{t'}}{\langle I(q,t')\rangle^2_{t'}}. \tag{1}$$

$I(q,t')$ is the intensity at time t' and the modulus of the wave vector transfer $q \equiv |\mathbf{q}| = 4\pi \sin(\theta/2)/\lambda$, with wavelength λ and scattering angle θ. The g_2 function is related to the intermediate scattering function $f(q,t)$ and can be modeled in many cases by a Kohlrausch–Williams–Watts (KWW) expression

$$g_2(q,t) = 1 + \beta|f(q,t)|^2 = 1 + \beta \exp(-2(t/\tau)^{\gamma}). \tag{2}$$

Here, β is the speckle contrast defined by coherence properties of the x-ray beam and setup parameters, τ the characteristic relaxation time, and γ the KWW exponent. The q-dependence of $\tau \propto q^{-p}$ and the KWW exponent γ define the type of dynamics, e.g., diffusion results in $p = 2$ and $\gamma = 1$. In the case of two relaxations, Eq. (2) can be extended to

$$f(q,t) = b_1 \exp(-(t/\tau_1)^{\gamma_1}) + b_2 \exp(-(t/\tau_2)^{\gamma_2}). \tag{3}$$

Compared to commonly performed microscopy experiments, scattering experiments such as this XPCS study allow measurement of the dynamics of smaller particles. This has several advantages such as low or at least negligible influence of gravity on the sample. The time scale of colloidal systems is given by the Brownian time $\tau_B = r^2/D \propto r^3$, where D denotes the diffusion constant. Consequently, a reduction of the particle radius by one order of magnitude enables studying three orders of magnitude longer in units of τ_B. Assuming a hydrodynamic radius as the sum of the radius of the gold particles and the PEG ligand length of $r_{total} = 16$ nm, we obtain a Brownian time of $\tau_B \approx 21$ μs for $T = 290$ K. This corresponds to a total studied time window of about $(5 \times 10^8)\tau_B$, i.e., 3 years of experimental time using a particle radius of 1 μm, which is a standard size in microscopy. Using fluorescence microscopy, smaller sizes can be accessed;[41] however, the radii are still an order of magnitude larger than in our study.

III. RESULTS

Figure 1 shows g_2 functions for $q = 0.023$ nm^{-1} at different experimental times t_w. $t_w = 0$ refers to the start of cooling and start

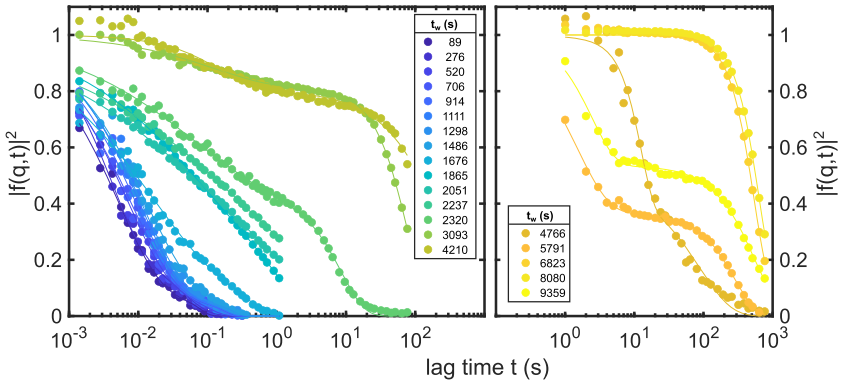

FIG. 1. Correlation functions g_2 at $q = 0.023$ nm^{-1}. In the left panel, data are shown from the same sample spot, the right panel shows data from different spots for large t_w. Lines are fits to Eq. (2) for single decays and to Eq. (3) for double decays.

of XPCS runs. For $t_w < 4300$ s, the data shown were measured at the same sample spot within the cycling measurements over ten spots. With decreasing temperature, the dynamics slow down due to the increasing viscosity of the solvent. Around $t_w \approx 1600$ s, the relaxation time increases sharply and the correlation functions become increasingly stretched. Finally, a slow and less stretched secondary decay appears. Note that such a second decay is only modeled, if $b_2 > 0.1$ in Eq. (3); otherwise, a single decay with only one relaxation time is considered. XPCS studies on colloidal gels frequently report missing speckle contrasts for $t \to 0$, which arise due to particle motions faster than the experimental time resolution.[22,26,42–44] In contrast to those studies, we can model the whole g_2 function and also track the fast dynamics because of the quality of the data and the high repetition rate of the detector.

In general, the dynamics suggest a transition from a fluid to an arrested state, i.e., a colloidal gel in this case.[22] The latter state is characterized by different time scales that are associated with slow structural relaxation and faster rattling, e.g., particle moving within the cage formed by its next-neighbors. During gelation, the faster process appears to be very heterogeneous due to superposition of multiple dynamic modes[10,45] as indicated by the small KWW exponent. At later t_w, slower decay dominates and the dynamics partially depend on the actual position of the sample as evidenced by the different relaxations observed for $t_w > 4600$ s (right panel of Fig. 1). Note that these fluctuations may also be temporal ones, or a combination of both, as frequently observed in aging gels.[21]

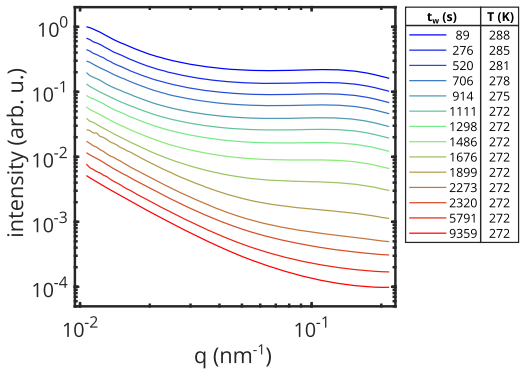

FIG. 2. Intensity $I(q)$ from one sample spot. The lines are vertically offset for clarity.

The transition of dynamics is connected to a change of structure as expressed by the SAXS signal $I(q)$ shown in Fig. 2 for one sample spot at selected t_w. During cooling to 272 K, $I(q)$ does not vary. After reaching 272 K and after expiration of another ~600 s, the intensity changes with increasing contribution at low q simultaneous to the slowdown of dynamics. This is a fingerprint of formation of larger domains such as network structures found in attractive gels. After about $t_w = 2300$ s, the average structure does not change significantly anymore.

Next, we want to discuss dynamical and structural changes quantitatively. The relaxation times τ obtained from the fits of the g_2 functions to the data are shown in Fig. 3 (top). Here, results are shown for all studied t_w at $q = 0.023$ nm^{-1}, i.e., for all studied sample spots. For small t_w, τ increases slowly due to increasing viscosity. This is highlighted by the black line showing the relaxation time of diffusing particles in water with a radius of 16 nm, i.e., the sum of gold core and PEG ligand. Around $t_w \approx 1600$ s, the relaxation time increases sharply as discussed above. With further increase in t_w at fixed $T = 272$ K, the relaxation time increases continuously, which indicates aging of the gel.[20,22] If a second decay of the correlation function is modeled, the fast relaxation time is displayed by open triangles. Overall, we find two branches for the fast and slow relaxation, both slowing down in parallel toward 10^3 and 10^1 s, respectively, and only small differences for different sample spots.

As we have access to the low-q regime in the USAXS-type experiments, we determine the characteristic length scale ξ in our sample from the $I(q)$ using the Ornstein–Zernike equation,[46]

$$I(q) = \frac{I_0}{1 + q^2\xi^2}, \tag{4}$$

where I_0 is a scaling parameter. In many cases, a modified version is used including the fractal dimension δ.[46–48] As we found that $1.5 \lesssim \delta \lesssim 2.5$ for all t_w, Eq. (4) is used here, which sets $\delta = 2$. The corresponding fits are shown in the supplementary material. The resulting ξ is shown in Fig. 3 (bottom), comparing the slowdown of dynamics with quantitative structural properties. At small t_w, we find $\xi \approx 130$ nm, with small variation depending on the sample spot. Similar to the trend observed for dynamics, ξ increases steeply around

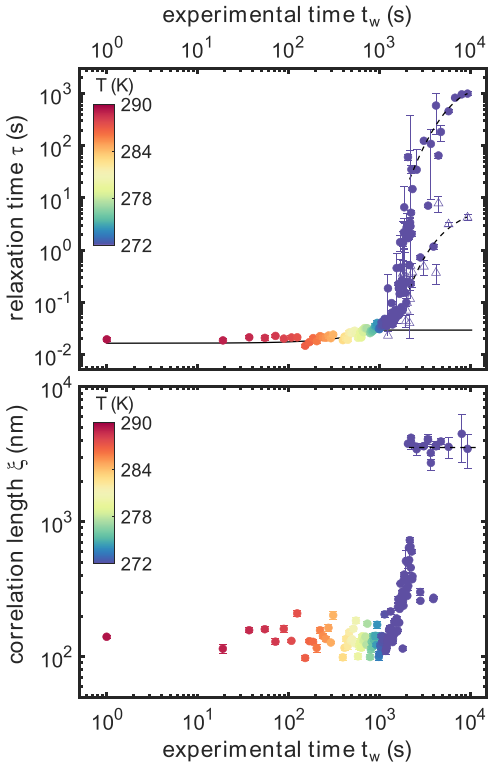

FIG. 3. Relaxation times τ (top) at $q = 0.023$ nm^{-1} and correlation length ξ (bottom) as function of t_w for all the studied XPCS runs. The temperature is encoded by the color of the data points. The solid line represents the relaxation time for free diffusion of spheres with a radius of 16 nm at the corresponding temperature, dashed lines are guide to the eyes. The open triangles in the top figure are used for the faster relaxation time in case a two-step correlation function was found.

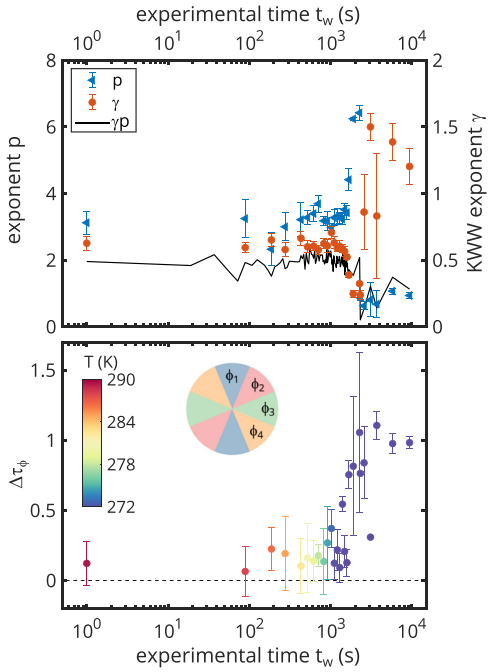

FIG. 4. Top: Exponents p and γ as function of t_w shown for two spots on the sample. The solid line is the product γp for all measurements. Bottom: Degree of direction-dependent dynamics $\Delta\tau_\phi$ as function of t_w. The temperature is encoded by the color of the data points. The inset shows a scheme of the ϕ regions on the detector with an angular width of $\pi/4$. Results were averaged for regions with the same color.

$t_w \approx 1600$ s and saturates at $\xi_{max} \approx 3700$ nm. This is a fingerprint of the formation of network structures and agglomerates as found in attractive gels. However, while τ shows aging, the correlation length ξ stays constant at this maximum value after the abrupt increase. This suggests that the slowdown of the dynamics and the increase of correlation length take place at the same time; however, in the gel state the dynamics is characterized by aging, while the structure is changed immediately.

The type of dynamics during gelation is further investigated by the q-dependence of the correlation time and the shape of the correlation functions. This is done by taking a closer look on the exponents p and γ shown in Fig. 4 (top) exemplary for two spots on the sample. For high t_w, we display the parameters of the dominant, slower relaxation process. In the beginning of the experiment, we find $p \approx 3$ (see also fits in the supplementary material) and $\gamma \approx 0.6$ to 0.7. This suggests sub-diffusive structural dynamics, which has been reported in other soft colloidal fluids where the ligand shell dominates the dynamics[49,50] as well as polymer-dominated composite materials.[51,52] On approaching the gelation point, p increases strongly up to $p \gtrsim 6$, while γ decreases well below 0.5. This stretching as well as the large value of p suggests an increasingly sub-diffusive nature of the dynamics toward confined diffusion when the gelation takes place. A similar general behavior has been reported close to colloidal glass transitions.[27,50,53,54] Anomalous dynamics with $p \approx 3$ have also been reported during gelation of soft particles;[10] however, extreme values like $p \approx 6$ were found uniquely in our study and may indicate a feature of gel transitions.

The product $p\gamma$ allows for further categorization of dynamical regimes. In particular, $p\gamma \approx 2$ is found for liquids and $p\gamma \lesssim 2$ for arrested states as shown for colloidal soft spheres.[54] We find such a transition around $t_w \approx 2000$ s, coinciding with $p \gtrsim 6$ and the drop of γ. At larger t_w in the gel state, we obtained $\gamma \approx 1.5$ and $p \approx 1$. Such exponents have been reported in the last two decades for many different out-of-equilibrium systems, especially gels,[20,55–58] and is connected to stress-dominated dynamics. Note that the impact of aging on the correlation functions can be neglected in most of our data thanks to the short runs taken. This is further shown by performing a two-time correlation analysis for $t_w > 2000$ s in the supplementary material.

In our previous study,[22] we reported anisotropic dynamics in the gel state. In order to check for such anisotropies, we performed a direction-dependent analysis of the dynamics. Such direction-dependent dynamics are usually reported for flowing systems[59,60] as well as during the recovery of 3D printing[61] and for the dynamics of aligned isotropic particles.[62] Studies on anisotropic gel dynamics are scarce and focused on two-dimensional gels[57] and the failure of the gel under load.[63] To detect anisotropic dynamics in our XPCS

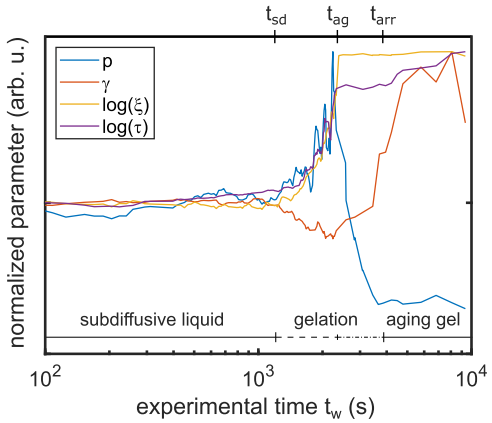

FIG. 5. Exponents p and γ compared to $\log(\xi)$ and $\log(\tau)$. For clarity, data are smoothed and normalized to the first value at $t_w = 1$ s as well as to their maximum. The resulting states are indicated.

data, g_2-functions were calculated for four different directions of the speckle pattern, each with a width of $\pi/4$ and periodicity of π. The directions on the speckle pattern are schematically demonstrated in the inset in Fig. 4 (bottom). To quantify the anisotropy of dynamics, the spread of the direction-dependent relaxation times τ_ϕ is calculated via $\Delta\tau_\phi = \frac{\max(\tau(\phi))-\min(\tau(\phi))}{\langle\tau(\phi)\rangle_\phi}$ and shown in Fig. 4 (bottom). We find that $\Delta\tau_\phi \approx 0$ within the error bars for the fluid state. In contrast, $\Delta\tau_\phi$ increases rapidly during gelation and reaches 1 in the gel state. This indicates that the gel is governed by a direction-dependence of the dynamics, which is absent for the colloidal fluid.

IV. CONCLUSION

Our observations on the gelation of PEGylated gold nanoparticles are summarized in Fig. 5 where all the parameters discussed above are qualitatively compared. The overall picture suggests a complex gelation transition. First, in the fluid state, the dynamics are sub-diffusive, with a relaxation time that decreases slightly with cooling due to the increasing viscosity of the solvent. The average structure obtained by SAXS does not vary.

Second, after crossing T_{gel}, the relaxation time continuously increases and grows by up to four orders of magnitude until around $t_w \approx 2000$ s, when the gel is formed. Furthermore, this slowdown is associated with the appearance of a secondary relaxation, suggesting the existence of two dynamical regimes. In glasses, this is typically associated with α- and β-relaxations, describing the (fast) movement of a particle within the cage formed by its neighbors and the (slow) break-out out of the cages. In the gel and glass states, the latter state becomes more and more unlikely; thus, the second relaxation time increases and eventually the system becomes non-ergodic. Simultaneous to the increase in relaxation time, the Ornstein–Zernike correlation length grows discontinuously above 3 μm. Most interestingly, the structure changes rapidly while the dynamics undergo aging and seem to settle just around $t_w \approx 10^4$ s. Note that the actual time of the transitions and the gel dynamics are similar but not identical for all sample spots. Interestingly, the growth rate of τ and ξ also increases; so, both cannot be modeled by a power law as, e.g., done in microscopy studies of aging gels.[64]

Third, the gelation is characterized by a strong increase of the exponent p. This can be further visualized by comparing XPCS results with the mean-square displacement (MSD), typically studied in microscopy and theory. The observed q^{-6} scaling of the relaxation time around the gelation point corresponds to a MSD scaling of $t^{1/3}$.[65] Such extreme anomalous, sub-diffusive dynamics underlines the transition from free diffusion to confined, rattling dynamics. Furthermore, γ decreases to 0.2, indicating a high degree of heterogeneous dynamics during gelation. This can be understood as the result of averaging over regions with different, likely exponential dynamics.[10] Together with the spatial dependence of dynamics, this may be a fingerprint of network formation.[17] Afterward, while the relaxation time is governed by aging, both exponents show a behavior toward hyperdiffusive, ballistic dynamics ($p \approx 1, \gamma \approx 1.5$) typically found for arrested states.[20]

Fourth, the gel is characterized by non-isotropic dynamics. The onset of direction-dependence of the dynamics coincides with the onset of gelation. Its degree quantified by $\Delta\tau_\phi$ increases with t_w and reaches a constant value after $t_w \approx 4000$ s. Such non-isotropic hyperdiffusive dynamics have been recently reported in glasses and gels.[22,66] They are associated with stress-driven relaxation of mobile regions in arrested systems. Our results provide further experimental support for this and connect the onset of anisotropy of dynamics with an increasing correlation length and further dynamical properties.

Our investigation of structure and dynamics by XPCS during gelation indicates a three-step gelation process that is characterized by three characteristic times (see Fig. 5). At $t_{sd} \approx 1600$ s, the gelation starts, manifested by rapid increase of both the relaxation time and correlation length. In addition, the dynamics become non-isotropic and extremely superdiffusive. Note that this onset of gelation takes place after the sample rested about 10 min at 272 K within the stability region of the gel. This delay may be connected to the low volume fractions studied. Following the gelation picture proposed by Ref. 17, clusters need to become compact before eventually connecting into a percolating structure leading to the rapid slowdown. Around $t_{ag} \approx 2400$ s, the correlation length settles at its maximum and the mean structure does not change afterward. The dynamics are still characterized by aging, i.e., τ slows down continuously. In parallel, p decreases from $p \approx 6$ toward $p \approx 1$, while γ increases from 0.2 to above 1. Finally, at $t_{arr} \approx 4000$ s, the aging slows down further while the exponents p and γ have reached values that can be associated with an arrested gel state.

Thanks to the smaller particle size used in our scattering study compared to conventional microscopy experiments, we could access the structure and dynamics over a very broad time window. Note that the Brownian time τ_B should be measured by XPCS at a q-value of $q = 2\pi/r \approx 0.39$ nm^{-1}. Considering the q-dependence of $\tau \propto q^{-1}$ at large t_w, this corresponds to an effectively larger τ at the q-value focused on in this work of $\tau(q = 0.023\ \text{nm}^{-1}) \approx 17\tau_B$. Thus, we covered an effective time range of gelation of up to $3 \times 10^7\,\tau_B$ with a time resolution of the q-scaled Brownian time of few ms.

Our study shows a very rich picture of the structure and dynamics during the gelation of PEGylated gold particles. The three-step process shows that first the structure is established, then the dynamics follow, showing spatial heterogeneities and anomalous

behavior, such as anisotropy and strong superdiffusivity, that can be connected to stress release. Owing to the recent development of next-generation x-ray light sources, we expect that XPCS will enable similar investigations on the relevant length scales of soft matter and complex fluids[40] without *a priori* limitations on the sample structure or morphology.

SUPPLEMENTARY MATERIAL

See the supplementary material for details on cooling rates, analysis of $I(q)$, relaxation times, and two-time correlations.

ACKNOWLEDGMENTS

The authors thank DESY (Hamburg, Germany), a member of the Helmholtz Association HGF, for the provision of experimental facilities. Parts of this research were carried out at PETRA III. The authors thank Michael Sprung for assistance with using the P10 beamline.

This research used beamline CHX (11-ID) of the National Synchrotron Light Source II, a U.S. Department of Energy (DOE) Office of Science User Facility operated for the DOE Office of Science by Brookhaven National Laboratory under Contract No. DE-SC0012704. We thank Lutz Wiegart and Andrei Fluerasu for their assistance.

This work was financially supported by DESY, a member of the Helmholtz Association (HGF), and by the Cluster of Excellence "Advanced Imaging of Matter" of the Deutsche Forschungsgemeinschaft (DFG)—EXC 2056—Project ID No. 390715994.

AUTHOR DECLARATIONS

Conflict of Interest

The authors have no conflicts to disclose.

Author Contributions

Avni Jain: Conceptualization (lead); Data curation (lead); Formal analysis (supporting); Investigation (equal); Methodology (equal); Validation (equal); Writing – review & editing (equal). **Florian Schulz**: Data curation (equal); Investigation (equal); Resources (lead); Writing – review & editing (equal). **Francesco Dallari**: Data curation (equal); Formal analysis (supporting); Investigation (equal); Writing – review & editing (equal). **Verena Markmann**: Data curation (equal); Investigation (equal); Writing – review & editing (equal). **Fabian Westermeier**: Investigation (equal); Resources (equal); Software (equal); Writing – review & editing (equal). **Yugang Zhang**: Investigation (equal); Resources (equal); Software (equal); Writing – review & editing (equal). **Gerhard Grübel**: Conceptualization (equal); Funding acquisition (equal); Supervision (equal); Writing – review & editing (equal). **Felix Lehmkühler**: Conceptualization (equal); Data curation (equal); Formal analysis (lead); Funding acquisition (equal); Investigation (equal); Methodology (equal); Project administration (equal); Supervision (equal); Validation (equal); Visualization (lead); Writing – original draft (lead); Writing – review & editing (equal).

DATA AVAILABILITY

The data that support the findings of this study are available from the corresponding author upon reasonable request.

REFERENCES

[1] V. Trappe and P. Sandkühler, "Colloidal gels—Low-density disordered solid-like states," Curr. Opin. Colloid Interface Sci. **8**, 494–500 (2004).
[2] E. Zaccarelli, "Colloidal gels: Equilibrium and non-equilibrium routes," J. Phys.: Condens. Matter **19**, 323101 (2007).
[3] L. Berthier and G. Biroli, "Theoretical perspective on the glass transition and amorphous materials," Rev. Mod. Phys. **83**, 587–645 (2011).
[4] G. L. Hunter and E. R. Weeks, "The physics of the colloidal glass transition," Rep. Prog. Phys. **75**, 066501 (2012).
[5] A. Coniglio, T. Abete, A. de Candia, E. Del Gado, and A. Fierro, "Dynamical heterogeneities: From glasses to gels," J. Phys.: Condens. Matter **20**, 494239 (2008).
[6] *Dynamical Heterogeneities in Glasses, Colloids, and Granular Media*, edited by L. Berthier, G. Biroli, J.-P. Bouchaud, L. Cipelletti, and W. van Saarloos (Oxford University Press, 2011).
[7] I. Tah, A. Mutneja, and S. Karmakar, "Understanding slow and heterogeneous dynamics in model supercooled glass-forming liquids," ACS Omega **6**, 7229–7239 (2021).
[8] A. M. Puertas, M. Fuchs, and M. E. Cates, "Dynamical heterogeneities close to a colloidal gel," J. Chem. Phys. **121**, 2813 (2004).
[9] C. P. Royall, M. A. Faers, S. L. Fussell, and J. E. Hallett, "Real space analysis of colloidal gels: Triumphs, challenges and future directions," J. Phys.: Condens. Matter **33**, 453002 (2021).
[10] J. H. Cho, R. Cerbino, and I. Bischofberger, "Emergence of multiscale dynamics in colloidal gels," Phys. Rev. Lett. **124**, 088005 (2020).
[11] M. E. Cates, M. Fuchs, K. Kroy, W. C. K. Poon, and A. M. Puertas, "Theory and simulation of gelation, arrest and yielding in attracting colloids," J. Phys.: Condens. Matter **16**, S4861–S4875 (2004).
[12] S. Manley, H. M. Wyss, K. Miyazaki, J. C. Conrad, V. Trappe, L. J. Kaufman, D. R. Reichman, and D. A. Weitz, "Glasslike arrest in spinodal decomposition as a route to colloidal gelation," Phys. Rev. Lett. **95**, 238302 (2005).
[13] P. J. Lu, E. Zaccarelli, F. Ciulla, A. B. Schofield, F. Sciortino, and D. A. Weitz, "Gelation of particles with short-range attraction," Nature **453**, 499–503 (2008).
[14] A. P. R. Eberle, N. J. Wagner, and R. Castañeda-Priego, "Dynamical arrest transition in nanoparticle dispersions with short-range interactions," Phys. Rev. Lett. **106**, 105704 (2011).
[15] C. P. Royall, S. R. Williams, and H. Tanaka, "Vitrification and gelation in sticky spheres," J. Chem. Phys. **148**, 044501 (2018).
[16] M. Kohl, R. F. Capellmann, M. Laurati, S. U. Egelhaaf, and M. Schmiedeberg, "Directed percolation identified as equilibrium pre-transition towards non-equilibrium arrested gel states," Nat. Commun. **7**, 11817 (2016).
[17] H. Tsurusawa, M. Leocmach, J. Russo, and H. Tanaka, "Direct link between mechanical stability in gels and percolation of isostatic particles," Sci. Adv. **5**, eaav6090 (2019).
[18] S. Zhang, L. Zhang, M. Bouzid, D. Z. Rocklin, E. Del Gado, and X. Mao, "Correlated rigidity percolation and colloidal gels," Phys. Rev. Lett. **123**, 058001 (2019).
[19] M. Tateno, T. Yanagishima, and H. Tanaka, "Microscopic structural origin behind slowing down of colloidal phase separation approaching gelation," J. Chem. Phys. **156**, 084904 (2022).
[20] L. Cipelletti, S. Manley, R. C. Ball, and D. A. Weitz, "Universal aging features in the restructuring of fractal colloidal gels," Phys. Rev. Lett. **84**, 2275–2278 (2000).
[21] Z. Filiberti, R. Piazza, and S. Buzzaccaro, "Multiscale relaxation in aging colloidal gels: From localized plastic events to system-spanning quakes," Phys. Rev. E **100**, 042607 (2019).
[22] A. Jain, F. Schulz, I. Lokteva, L. Frenzel, G. Grübel, and F. Lehmkühler, "Anisotropic and heterogeneous dynamics in an aging colloidal gel," Soft Matter **16**, 2864–2872 (2020).

[23]Q. Zhang, D. Bahadur, E. M. Dufresne, P. Grybos, P. Kmon, R. L. Leheny, P. Maj, S. Narayanan, R. Szczygiel, S. Ramakrishnan, and A. Sandy, "Dynamic scaling of colloidal gel formation at intermediate concentrations," Phys. Rev. Lett. **119**, 178006 (2017).
[24]Q. Zhang, E. M. Dufresne, S. Narayanan, P. Maj, A. Koziol, R. Szczygiel, P. Grybos, M. Sutton, and A. R. Sandy, "Sub-microsecond-resolved multi-speckle x-ray photon correlation spectroscopy with a pixel array detector," J. Synchrotron Radiat. **25**, 1408–1416 (2018).
[25]J. Möller, M. Sprung, A. Madsen, and C. Gutt, "X-ray photon correlation spectroscopy of protein dynamics at nearly diffraction-limited storage rings," IUCrJ **6**, 794–803 (2019).
[26]Y. Chen, S. A. Rogers, S. Narayanan, J. L. Harden, and R. L. Leheny, "Microscopic ergodicity breaking governs the emergence and evolution of elasticity in glass-forming nanoclay suspensions," Phys. Rev. E **102**, 042619 (2020).
[27]F. Lehmkühler, B. Hankiewicz, M. A. Schroer, L. Müller, B. Ruta, D. Sheyfer, M. Sprung, K. Tono, T. Katayama, M. Yabashi, T. Ishikawa, C. Gutt, and G. Grübel, "Slowing down of dynamics and orientational order preceding crystallization in hard-sphere systems," Sci. Adv. **6**, eabc5916 (2020).
[28]D. Sheyfer, Q. Zhang, J. Lal, T. Loeffler, E. M. Dufresne, A. R. Sandy, S. Narayanan, S. K. R. S. Sankaranarayanan, R. Szczygiel, P. Maj, L. Soderholm, M. R. Antonio, and G. B. Stephenson, "Nanoscale critical phenomena in a complex fluid studied by x-ray photon correlation spectroscopy," Phys. Rev. Lett. **125**, 125504 (2020).
[29]W. Jo, F. Westermeier, R. Rysov, O. Leupold, F. Schulz, S. Tober, V. Markmann, M. Sprung, A. Ricci, T. Laurus, A. Aschkan, A. Klyuev, U. Trunk, H. Graafsma, G. Grübel, and W. Roseker, "Nanosecond x-ray photon correlation spectroscopy using pulse time structure of a storage-ring source," IUCrJ **8**, 124–130 (2021).
[30]F. Dallari, A. Jain, M. Sikorski, J. Möller, R. Bean, U. Boesenberg, L. Frenzel, C. Goy, J. Hallmann, Y. Kim, I. Lokteva, V. Markmann, G. Mills, A. Rodriguez-Fernandez, W. Roseker, M. Scholz, R. Shayduk, P. Vagovic, M. Walther, F. Westermeier, A. Madsen, A. P. Mancuso, G. Grübel, and F. Lehmkühler, "Microsecond hydrodynamic interactions in dense colloidal dispersions probed at the european XFEL," IUCrJ **8**, 775–783 (2021).
[31]A. Girelli, H. Rahmann, N. Begam, A. Ragulskaya, M. Reiser, S. Chandran, F. Westermeier, M. Sprung, F. Zhang, C. Gutt, and F. Schreiber, "Microscopic dynamics of liquid-liquid phase separation and domain coarsening in a protein solution revealed by x-ray photon correlation spectroscopy," Phys. Rev. Lett. **126**, 138004 (2021).
[32]N. Begam, A. Ragulskaya, A. Girelli, H. Rahmann, S. Chandran, F. Westermeier, M. Reiser, M. Sprung, F. Zhang, C. Gutt, and F. Schreiber, "Kinetics of network formation and heterogeneous dynamics of an egg white gel revealed by coherent x-ray scattering," Phys. Rev. Lett. **126**, 098001 (2021).
[33]F. Schulz, T. Homolka, N. G. Bastús, V. Puntes, H. Weller, and T. Vossmeyer, "Little adjustments significantly improve the turkevich synthesis of gold nanoparticles," Langmuir **30**, 10779–10784 (2014).
[34]F. Schulz, G. T. Dahl, S. Besztejan, M. A. Schroer, F. Lehmkühler, G. Grübel, T. Vossmeyer, and H. Lange, "Ligand layer engineering to control stability and interfacial properties of nanoparticles," Langmuir **32**, 7897–7907 (2016).
[35]F. Schulz, J. Möller, F. Lehmkühler, A. J. Smith, T. Vossmeyer, H. Lange, G. Grübel, and M. A. Schroer, "Structure and stability of PEG- and mixed PEG-layer-coated nanoparticles at high particle concentrations studied in situ by small-angle x-ray scattering," Part. Part. Syst. Charact. **35**, 1700319 (2018).
[36]A. Duri, H. Bissig, V. Trappe, and L. Cipelletti, "Time-resolved-correlation measurements of temporally heterogeneous dynamics," Phys. Rev. E **72**, 051401 (2005).
[37]G. Grübel, A. Madsen, and A. Robert, "X-ray photon correlation spectroscopy (XPCS)," in *Soft Matter Characterization* (Springer, Netherlands, 2008), pp. 953–995.
[38]A. R. Sandy, Q. Zhang, and L. B. Lurio, "Hard x-ray photon correlation spectroscopy methods for materials studies," Ann. Rev. Mater. Res. **48**, 167–190 (2018).
[39]A. Madsen, A. Fluerasu, and B. Ruta, "Structural dynamics of materials probed by x-ray photon correlation spectroscopy," in *Synchrotron Light Sources and Free-Electron Lasers* (Springer International Publishing, 2020), pp. 1989–2018.
[40]F. Lehmkühler, W. Roseker, and G. Grübel, "From femtoseconds to hours—Measuring dynamics over 18 orders of magnitude with coherent x-rays," Appl. Sci. **11**, 6179 (2021).
[41]J. E. Hallett, F. Turci, and C. P. Royall, "Local structure in deeply supercooled liquids exhibits growing lengthscales and dynamical correlations," Nat. Commun. **9**, 3272 (2018).
[42]R. Bandyopadhyay, D. Liang, H. Yardimci, D. A. Sessoms, M. A. Borthwick, S. G. J. Mochrie, J. L. Harden, and R. L. Leheny, "Evolution of particle-scale dynamics in an aging clay suspension," Phys. Rev. Lett. **93**, 228302 (2004).
[43]X. Lu, S. G. Mochrie, S. Narayanan, A. R. Sandy, and M. Sprung, "How a liquid becomes a glass both on cooling and on heating," Phys. Rev. Lett. **100**, 045701 (2008).
[44]J. L. Harden, H. Guo, M. Bertrand, T. N. Shendruk, S. Ramakrishnan, and R. L. Leheny, "Enhanced gel formation in binary mixtures of nanocolloids with short-range attraction," J. Chem. Phys. **148**, 044902 (2018).
[45]A. H. Krall and D. A. Weitz, "Internal dynamics and elasticity of fractal colloidal gels," Phys. Rev. Lett. **80**, 778–781 (1998).
[46]L. Wang, G. Shan, and P. Pan, "Highly enhanced toughness of interpenetrating network hydrogel by incorporating poly(ethylene glycol) in first network," RSC Adv. **4**, 63513–63519 (2014).
[47]J. Bibette, T. G. Mason, H. Gang, and D. A. Weitz, "Kinetically induced ordering in gelation of emulsions," Phys. Rev. Lett. **69**, 981–984 (1992).
[48]M. Carpineti and M. Giglio, "Spinodal-type dynamics in fractal aggregation of colloidal clusters," Phys. Rev. Lett. **68**, 3327–3330 (1992).
[49]L. Frenzel, F. Lehmkühler, I. Lokteva, S. Narayanan, M. Sprung, and G. Grübel, "Anomalous dynamics of concentrated silica-PNIPAm nanogels," J. Phys. Chem. Lett. **10**, 5231–5236 (2019).
[50]L. Frenzel, M. Dartsch, G. M. Balaguer, F. Westermeier, G. Grübel, and F. Lehmkühler, "Glass-liquid and glass-gel transitions of soft-shell particles," Phys. Rev. E **104**, l012602 (2021).
[51]P. Falus, M. A. Borthwick, S. Narayanan, A. R. Sandy, and S. G. Mochrie, "Crossover from stretched to compressed exponential relaxations in a polymer-based sponge phase," Phys. Rev. Lett. **97**, 066102 (2006).
[52]R. Poling-Skutvik, K. I. S. Mongcopa, A. Faraone, S. Narayanan, J. C. Conrad, and R. Krishnamoorti, "Structure and dynamics of interacting nanoparticles in semidilute polymer solutions," Macromolecules **49**, 6568–6577 (2016).
[53]A. M. Philippe, D. Truzzolillo, J. Galvan-Myoshi, P. Dieudonné-George, V. Trappe, L. Berthier, and L. Cipelletti, "Glass transition of soft colloids," Phys. Rev. E **97**, 040601 (2018).
[54]V. Nigro, B. Ruzicka, B. Ruta, F. Zontone, M. Bertoldo, E. Buratti, and R. Angelini, "Relaxation dynamics, softness, and fragility of microgels with interpenetrated polymer networks," Macromolecules **53**, 1596–1603 (2020).
[55]H. Guo, S. Ramakrishnan, J. L. Harden, and R. L. Leheny, "Gel formation and aging in weakly attractive nanocolloid suspensions at intermediate concentrations," J. Chem. Phys. **135**, 154903 (2011).
[56]O. Czakkel and A. Madsen, "Evolution of dynamics and structure during formation of a cross-linked polymer gel," Europhys. Lett. **95**, 28001 (2011).
[57]D. Orsi, L. Cristofolini, G. Baldi, and A. Madsen, "Heterogeneous and anisotropic dynamics of a 2D gel," Phys. Rev. Lett. **108**, 105701 (2012).
[58]B. Ruta, O. Czakkel, Y. Chushkin, F. Pignon, R. Nervo, F. Zontone, and M. Rinaudo, "Silica nanoparticles as tracers of the gelation dynamics of a natural biopolymer physical gel," Soft Matter **10**, 4547 (2014).
[59]S. Busch, T. H. Jensen, Y. Chushkin, and A. Fluerasu, "Dynamics in shear flow studied by x-ray photon correlation spectroscopy," Eur. Phys. J. E **26**, 55–62 (2008).
[60]J. Möller and T. Narayanan, "Velocity fluctuations in sedimenting Brownian particles," Phys. Rev. Lett. **118**, 198001 (2017).
[61]K. J. Johnson, L. Wiegart, A. C. Abbott, E. B. Johnson, J. W. Baur, and H. Koerner, "In operando monitoring of dynamic recovery in 3D-printed thermoset nanocomposites by XPCS," Langmuir **35**, 8758–8768 (2019).
[62]A. Pal, T. Zinn, M. A. Kamal, T. Narayanan, and P. Schurtenberger, "Anomalous dynamics of magnetic anisotropic colloids studied by XPCS," Small **14**, 1802233 (2018).

[63]S. Aime, L. Ramos, and L. Cipelletti, "Microscopic dynamics and failure precursors of a gel under mechanical load," Proc. Natl. Acad. Sci. U. S. A. **115**, 3587–3592 (2018).
[64]I. Zhang, C. P. Royall, M. A. Faers, and P. Bartlett, "Phase separation dynamics in colloid–polymer mixtures: The effect of interaction range," Soft Matter **9**, 2076 (2013).
[65]H. Guo, G. Bourret, R. B. Lennox, M. Sutton, J. L. Harden, and R. L. Leheny, "Entanglement-controlled subdiffusion of nanoparticles within concentrated polymer solutions," Phys. Rev. Lett. **109**, 055901 (2012).
[66]F. Dallari, A. Martinelli, F. Caporaletti, M. Sprung, G. Grübel, and G. Monaco, "Microscopic pathways for stress relaxation in repulsive colloidal glasses," Sci. Adv. **6**, eaaz2982 (2020).